

CH₃NH₃Cl-Assisted One-Step Solution Growth of CH₃NH₃PbI₃: Structure, Charge-Carrier Dynamics, and Photovoltaic Properties of Perovskite Solar Cells

Yixin Zhao and Kai Zhu*

Chemical and Materials Science Center, National Renewable Energy Laboratory, 15013 Denver West Parkway, Golden, Colorado 80401 (USA)

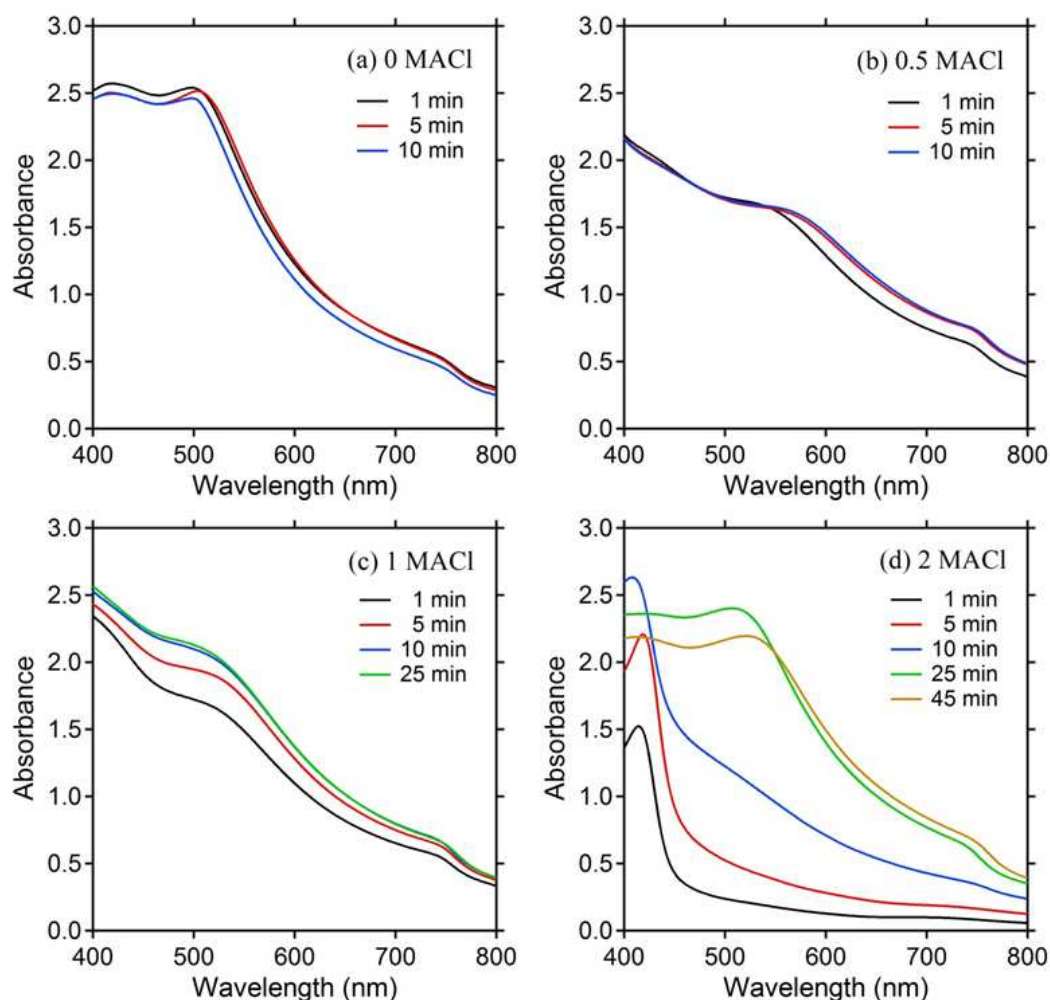


Figure S1. UV-vis absorption spectra of perovskite CH₃NH₃PbI₃ on mesoporous TiO₂ films as a function of annealing time at 100°C using precursors containing (a) 0 MACl, (b) 0.5 MACl, (c) 1 MACl, and (d) 2 MACl.

Table S1. Effect of MACl Amount (x) on Short-Circuit Photocurrent Density J_{sc} , Open-Circuit Voltage V_{oc} , Fill Factor FF, and Conversion Efficiency η of Solid-State Mesostructured (Meso) and Planar Perovskite $\text{CH}_3\text{NH}_3\text{PbI}_3$ Solar Cells. The mean values and standard deviations of the PV parameters from 12–20 cells for each type of devices are given in parentheses.

Cell Type (x)	J_{sc} (mA/cm^2)	V_{oc} (V)	FF	η (%)
Meso (0)	16.91 (16.96 \pm 0.64)	0.835 (0.826 \pm 0.013)	0.583 (0.545 \pm 0.032)	8.23 (7.64 \pm 0.64)
Meso (0.5)	18.55 (17.91 \pm 0.67)	0.845 (0.836 \pm 0.016)	0.582 (0.552 \pm 0.039)	9.12 (8.25 \pm 0.54)
Meso (1)	19.31 (19.44 \pm 0.61)	0.833 (0.824 \pm 0.019)	0.595 (0.565 \pm 0.023)	9.57 (9.03 \pm 0.33)
Meso (2)	19.48 (19.38 \pm 0.50)	0.829 (0.823 \pm 0.016)	0.625 (0.597 \pm 0.020)	10.09 (9.52 \pm 0.37)
Planar (0)	5.55 (4.75 \pm 0.82)	0.813 (0.735 \pm 0.060)	0.413 (0.375 \pm 0.035)	1.86 (1.34 \pm 0.39)
Planar (0.5)	17.90 (17.38 \pm 0.66)	1.004 (0.974 \pm 0.022)	0.607 (0.561 \pm 0.038)	10.91 (9.50 \pm 0.85)
Planar (1)	20.85 (20.08 \pm 0.76)	1.016 (1.019 \pm 0.029)	0.566 (0.515 \pm 0.048)	11.99 (10.51 \pm 0.92)
Planar (2)	20.36 (19.84 \pm 0.63)	1.023 (1.013 \pm 0.042)	0.581 (0.540 \pm 0.029)	12.10 (10.85 \pm 0.79)

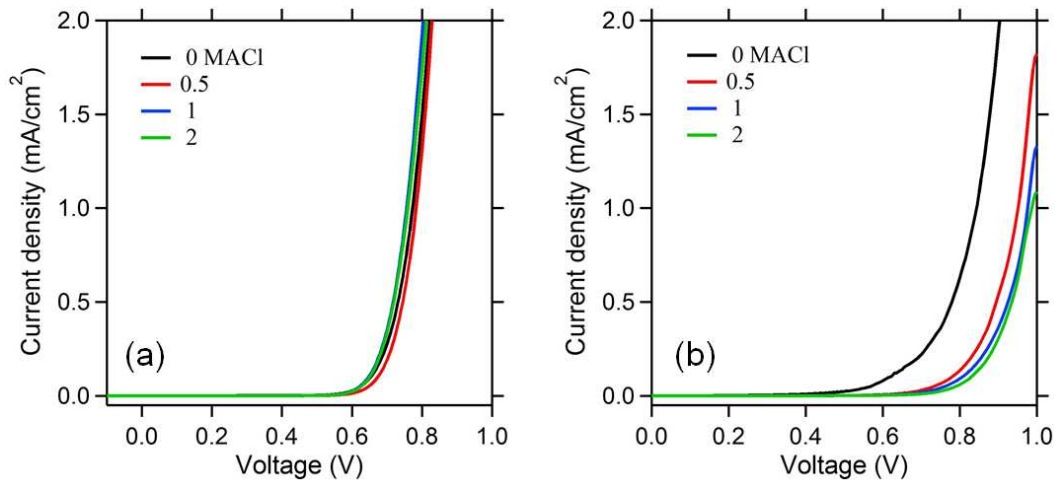


Figure S2. Dark J – V curves of (a) mesostructured and (b) planar perovskite solar cells as a function of added amount of MACl in the precursor solution for growing $\text{CH}_3\text{NH}_3\text{PbI}_3$.

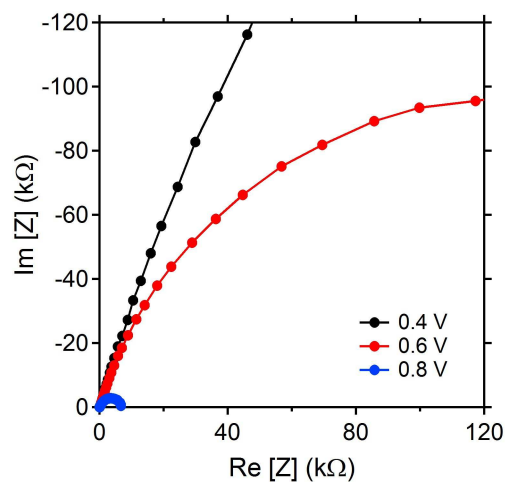


Figure S3. Typical Nyquist plots of the impedance responses for a planar perovskite cell with three different bias voltages. The model used for impedance analysis has been previously discussed by others.¹⁻²

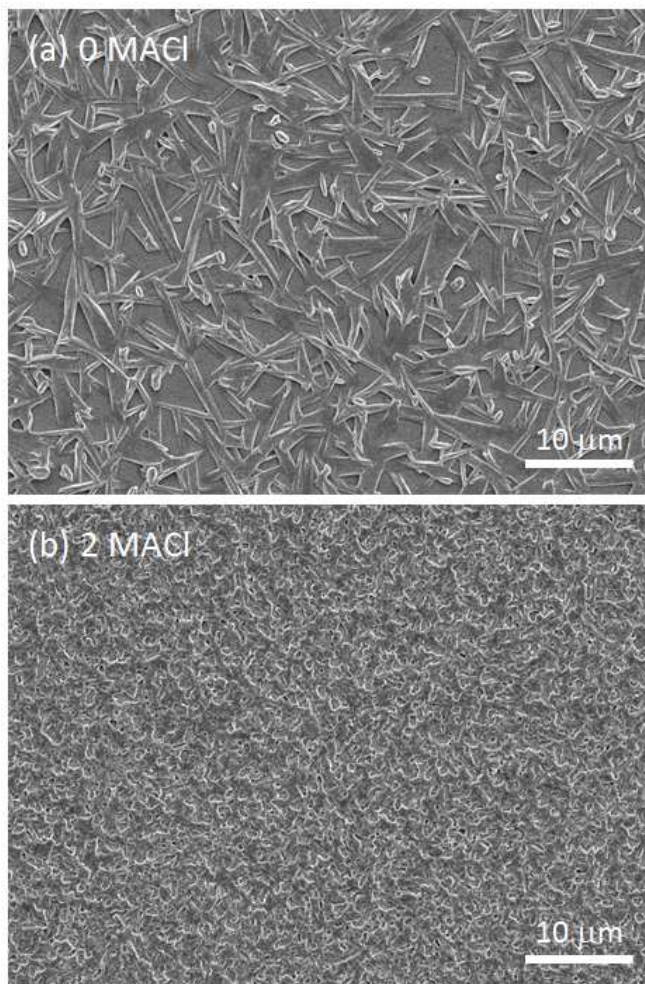


Figure S4. Typical large-scale SEM images of $\text{CH}_3\text{NH}_3\text{PbI}_3$ films grown on planar TiO_2 compact layer.

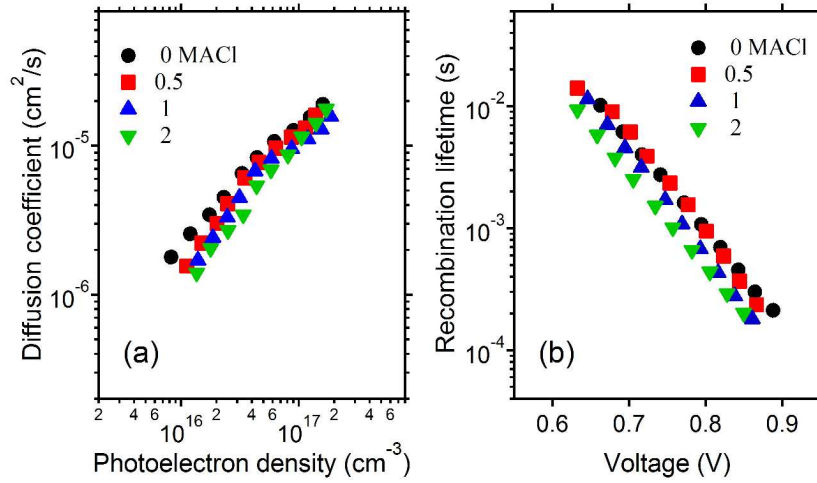


Figure S5. Effect of MACl on (a) electron diffusion coefficient as a function of photoelectron density and (b) recombination lifetime as function of voltage in mesostructured perovskite $\text{CH}_3\text{NH}_3\text{PbI}_3$ solar cells.

Charge transport and recombination properties in mesostructured perovskite $\text{CH}_3\text{NH}_3\text{PbI}_3$ solar cells are studied by IMPS and IMVS as described previously.³⁻⁴ Figure S5a shows the effect of using MACl on the diffusion coefficient (D) as a function of photoelectron density (n). All cells exhibit essentially the same power-law dependence ($D \propto n^{1/\alpha-1}$, with α being a disorder parameter) that is attributable to the electrons undergoing multiple trapping and detrapping through the mesoporous electrode film.⁵⁻¹⁰ There is no obvious difference of the D values for mesostructured perovskite cells using different amounts of MACl in the $\text{CH}_3\text{NH}_3\text{PbI}_3$ precursor solution, suggesting that using MACl does not affect the trap distribution on the TiO_2 surface. Similarly, no significant difference is observed for the recombination lifetime as a function of voltage for mesostructured cells prepared using different amounts of MACl (Figure S5b). These results imply that the charge collection (determined by the competition between transport and recombination) is not affected by the use of MACl.

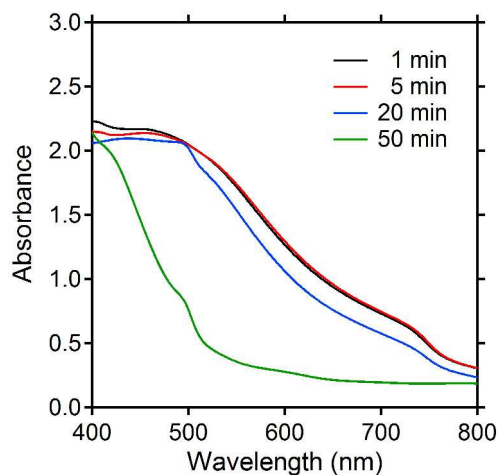


Figure S6. UV-vis absorption spectra of perovskite film as a function of annealing time at 100°C using a precursor containing equimolar mixture of MAI and PbI_2 .

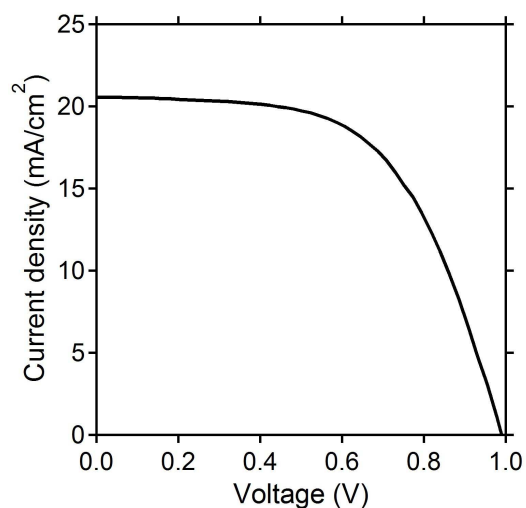


Figure S7. J - V curves of planar perovskite solar cell based on the mixed halide $\text{CH}_3\text{NH}_3\text{PbI}_{3-x}\text{Cl}_x$ prepared from the precursor containing MAI and PbCl_2 (3:1 molar ratio). The cell efficiency is 11.86% with a J_{sc} of 20.57 mA/cm^2 , V_{oc} of 0.995 V, and FF of 0.579.

REFERENCES

- (1). Juárez-Perez, E. J.; Wußler, M.; Fabregat-Santiago, F.; Lakus-Wollny, K.; Mankel, E.; Mayer, T.; Jaegermann, W.; Mora-Sero, I. Role of the Selective Contacts in the Performance of Lead Halide Perovskite Solar Cells. *J Phys. Chem. Lett.* **2014**, *5*, 680-685.
- (2). Christians, J. A.; Fung, R. C. M.; Kamat, P. V. An Inorganic Hole Conductor for Organo-Lead Halide Perovskite Solar Cells. Improved Hole Conductivity with Copper Iodide. *J. Am. Chem. Soc.* **2014**, *136*, 758-764.

- (3). Zhao, Y.; Zhu, K. Charge Transport and Recombination in Perovskite (CH₃NH₃)PbI₃ Sensitized TiO₂ Solar Cells. *J. Phys. Chem. Lett.* **2013**, *4*, 2880-2884.
- (4). Zhao, Y.; Nardes, A. M.; Zhu, K. Solid-State Mesostructured Perovskite CH₃NH₃PbI₃ Solar Cells: Charge Transport, Recombination, and Diffusion Length. *J. Phys. Chem. Lett.* **2014**, *5*, 490-494.
- (5). Nelson, J.; Haque, S. A.; Klug, D. R.; Durrant, J. R. Trap-Limited Recombination in Dye-Sensitized Nanocrystalline Metal Oxide Electrodes. *Phys. Rev. B* **2001**, *63*, 205321
- (6). Dloczik, L.; Ieperuma, O.; Lauermann, I.; Peter, L. M.; Ponomarev, E. A.; Redmond, G.; Shaw, N. J.; Uhlendorf, I. Dynamic Response of Dye-Sensitized Nanocrystalline Solar Cells: Characterization by Intensity-Modulated Photocurrent Spectroscopy. *J. Phys. Chem. B* **1997**, *101*, 10281-10289.
- (7). Solbrand, A.; Lindstrom, H.; Rensmo, H.; Hagfeldt, A.; Lindquist, S. E.; Sodergren, S. Electron Transport in the Nanostructured TiO₂-Electrolyte System Studied with Time-Resolved Photocurrents. *J. Phys. Chem. B* **1997**, *101*, 2514-2518.
- (8). Bisquert, J.; Vikhrenko, V. S. Interpretation of the Time Constants Measured by Kinetic Techniques in Nanostructured Semiconductor Electrodes and Dye-Sensitized Solar Cells. *J. Phys. Chem. B* **2004**, *108*, 2313-2322.
- (9). Barzykin, A. V.; Tachiya, M. Mechanism of Charge Recombination in Dye-Sensitized Nanocrystalline Semiconductors: Random Flight Model. *J. Phys. Chem. B* **2002**, *106*, 4356-4363.
- (10). Zhu, K.; Kopidakis, N.; Neale, N. R.; van de Lagemaat, J.; Frank, A. J. Influence of Surface Area on Charge Transport and Recombination in Dye-Sensitized TiO₂ Solar Cells. *J. Phys. Chem. B* **2006**, *110*, 25174-25180.